Theoretical and Spectroscopic Study of 2-Substituted Indan-1,3-diones: A Coherent Picture of the Tautomeric Equilibrium

5 AUTHORS, INCLUDING:

Silvia Angelova
Bulgarian Academy of Sciences
43 PUBLICATIONS **160** CITATIONS

SEE PROFILE

Venelin Enchev
Bulgarian Academy of Sciences
103 PUBLICATIONS **807** CITATIONS

SEE PROFILE

Marin Rogozherov
Bulgarian Academy of Sciences
19 PUBLICATIONS **108** CITATIONS

SEE PROFILE

Galya Ivanova
University of Porto
103 PUBLICATIONS **796** CITATIONS

SEE PROFILE

Theoretical and Spectroscopic Study of 2-Substituted Indan-1,3-diones: A Coherent Picture of the Tautomeric Equilibrium

Silvia Angelova, Venelin Enchev,* Kalina Kostova, Marin Rogojerov, and Galya Ivanova

Institute of Organic Chemistry, Bulgarian Academy of Sciences, 1113 Sofia, Bulgaria

Received: June 8, 2007; In Final Form: July 13, 2007

The structures of some 2-substituted indan-1,3-diones are investigated in the gas phase and solution using quantum chemical calculations and spectral (NMR, IR, and UV) measurements. The influence of the substituent at the 2-position on the tautomeric equilibrium of 2-substituted indan-1,3-diones in solvents with different polarity is evaluated. It is shown that the equilibrium in 2-formyl-indan-1,3-dione and 2-acetyl-indan-1,3-dione is shifted to the 2-hydroxyalkylidene-indan-1,3-dione tautomer, while 2-carboxyamide-indan-1,3-dione exists as a mixture of two tautomers, 2-(hydroxyaminomethylidene)-indan-1,3-dione and 2-carboamide-1-hydroxy-3-oxo-indan, with extremely fast proton transfer between them. The situation for 2-carboxy-indan-1,3-dione is quite different — on the basis of the analysis of the obtained results, the possible existence of an anionic form of 2-carboxy-indan-1,3-dione in solution can be inferred.

1. Introduction

There are a large number of investigations on the tautomeric equilibria of 1,3-dicarbonyl compounds[1] using a variety of techniques and carried out in water, in organic solvents, and recently in aqueous solutions (i) of surfactants forming micelles[2] and (ii) of cyclodextrins.[3] Many questions concerning the tautomerism of 1,3-dicarbonyl compounds have already been answered, but many others are still under investigation. Frequently, both the keto and the enol forms of many 1,3-dicarbonyl compounds are present in aqueous solutions in measurable proportions. The enol tautomers of 1,3-dicarbonyl compounds are stabilized by intramolecular hydrogen bonds; therefore the enol concentrations increase in aprotic solvents, i.e., when intermolecular hydrogen bonding with the solvent does not compete. This means that the keto–enol equilibrium is very sensitive to the nature of the solvent. 1,3-Diketones have one ionizable hydrogen atom, and the enolate form is present in alkaline medium, being in some cases the predominant species.[4]

In this work, we aim to check if theoretical calculations, supported by spectral (NMR, IR, and UV) measurements, can provide new information on the tautomerism of 2-substituted indan-1,3-diones. These compounds can exist in at least three tautomeric forms[5] and in five tautomeric forms if the substituent at position 2 is included in the process of tautomerization. We focus our attention on 2-formyl-indan-1,3-dione (**1**), 2-acetyl-indan-1,3-dione (**2**), 2-carboxy-indan-1,3-dione (**3**), and 2-carboxyamide-indan-1,3-dione (**4**), shown in Figure 1, and on the conversion between their most stable tautomers.

The physiological activity of 2-acetyl-indan-1,3-dione and its derivatives is well-documented.[6] Its structure has been studied by X-ray, IR, and NMR spectroscopies.[7–10] The tautomeric equilibrium in **2** has been investigated using quantum chemical calculations at the semiempirical[11] and ab initio[12] levels in the gas phase. According to the results obtained, 2-(1-hydroxyethylidene)-indan-1,3-dione, **2a**, (Figure 1) is the most stable. In our previous papers we have shown that intramolecular proton

TABLE 1: Calculated Relative Total Energies, ΔE_T, (kcal mol^{-1}) at Different Levels of Theory for Tautomers a–e of Compounds 1–4 Shown in Figure 1

	tautomer				
	a	**b**	**c**	**d**	**e**
1					
MP2/6-31G**	0.00	3.75	6.97		
MP4/6-31G**//MP2/6-31G**	0.00	4.25	5.11		
MP2/6-311G**	0.00	3.54			
MP4/6-311G**//MP2/6-311G**	0.00	4.07			
2					
MP2/6-31G**	0.00	4.11	6.63	28.44	21.92
MP4/6-31G**//MP2/6-31G**	0.00	4.26	4.63	28.77	19.87
MP2/6-311G**	0.00	3.68			
MP4/6-311G**//MP2/6-311G**	0.00	3.86			
3					
MP2/6-31G**	0.00	0.14	2.59		
MP4/6-31G**//MP2/6-31G**	0.07	0.00	0.58		
MP2/6-311G**	0.00	0.14			
MP4/6-311G**//MP2/6-311G**	0.05	0.00			
4					
MP2/6-31G**	0.00	0.93	5.28	13.65	20.83
MP4/6-31G**//MP2/6-31G**	0.00	0.74	3.38	14.02	18.52
MP2/6-311G**	0.00	0.92			
MP4/6-311G**//MP2/6-311G**	0.00	0.71			

transfer in **2** occurs in the singlet excited state,[11] and the compound is a promising sunscreen candidate.[13]

The syntheses of **4** was reported by Horton and Murdock in 1960,[14] but for a long time the structure of the compound was not elucidated. Recently we reported[15] that two tautomeric forms, 2-(hydroxyaminomethylidene)-indan-1,3-dione (**4a**) and 2-carboamide-1-hydroxy-3-oxo-indan (**4b**), are likely to coexist in the gas phase and in solution, with fast intramolecular proton transfer between them. In this paper, new IR and UV investigations and ab initio calculations in solution were carried out to elucidate the tautomeric composition of **4**.

2-Carboxy-indan-1,3-dione (**3**) was obtained by Perkin condensation of phthalic anhydride with acetic anhydride 130 years ago,[16,17] but its structure is still under debate.[17,18]

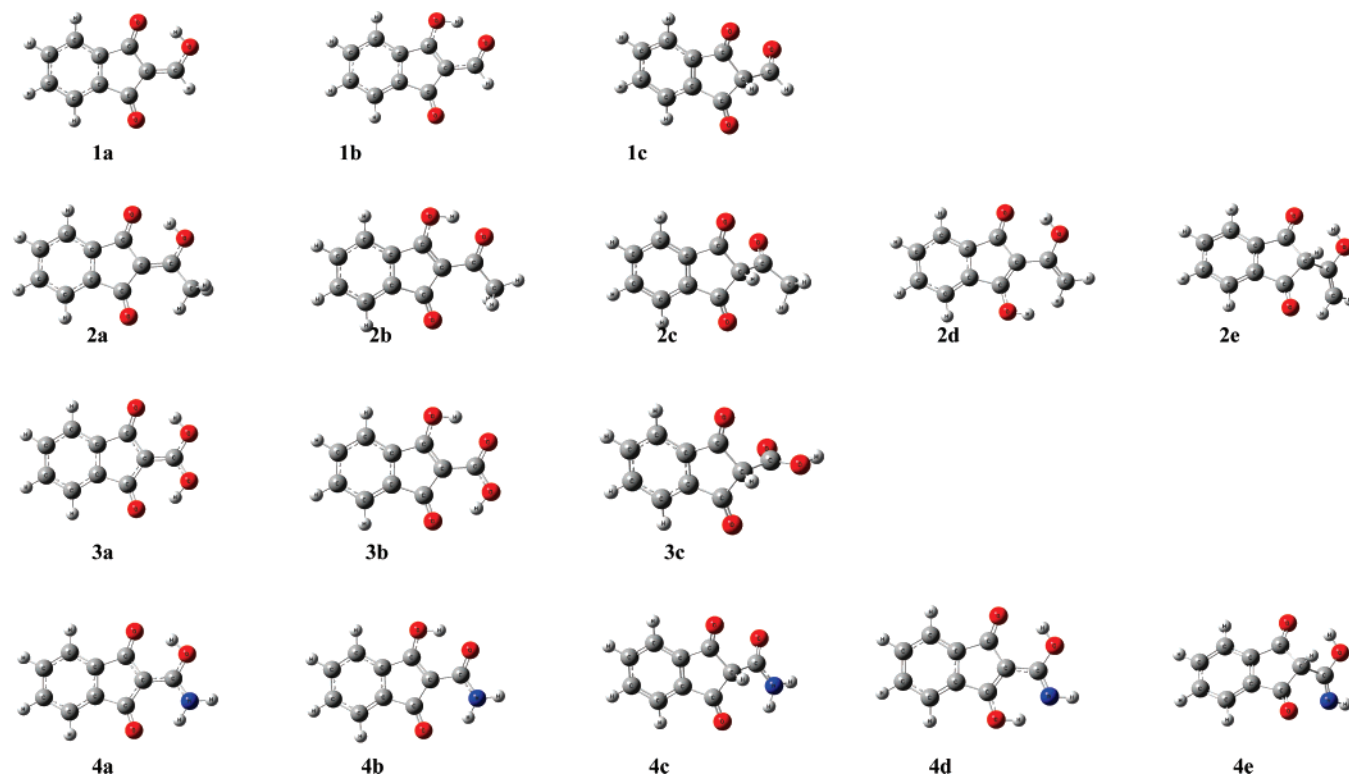* Author to whom correspondence should be addressed. Fax: ++359 2 8700225. E-mail: venelin@orgchm.bas.bg.

1a **1b** **1c**

2a **2b** **2c** **2d** **2e**

3a **3b** **3c**

4a **4b** **4c** **4d** **4e**

Figure 1. Tautomeric forms of 2-formylindan-1,3-dione, **1**, 2-acetylindan-1,3-dione, 2, 1,3-dioxoindane-2-carboxylic acid, **3**, and 1,3-dioxo-2-indancarboxamide, **4**, optimized at the MP2/6-31G** level of theory.

TABLE 2: Calculated Relative Enthalpies, Relative Gibbs Free Energies, and Activation Barriers (kcal mol^{-1}) for the Tautomers of Compounds 1−4 Shown in Figure 1 for Isolated Molecules and in CHCl$_3$ and DMSO Solution

	ΔH_0			$\Delta H_0^{\#}$		ΔG_{298}			$\Delta G_{298}^{\#}$	
compound	a	b	c	TS (a → b)	TS (a → c)	a	b	c	TS (a → b)	TS (a → c)
1										
MP2/6-31G**	0.00	3.20	5.74	3.81	59.15	0.00	3.23	4.83	3.97	59.07
MP4/6-31G**//MP2/6-31G**	0.00	3.70	3.88	5.83	62.12	0.00	3.73	2.97	6.15	62.03
PCM/MP4/6-31G**//MP2/6-31G**										
solvent CHCl$_3$	0.00	3.75	3.88	4.42		0.00	3.78	2.97	4.74	
solvent DMSO	0.00	3.87	3.77	4.50		0.00	3.90	2.86	4.81	
2										
MP2/6-31G**	0.00	3.62	5.97	3.38	56.38	0.00	3.61	5.53	3.71	56.40
MP4/6-31G**//MP2/6-31G**	0.00	3.78	3.97	5.04	58.85	0.00	3.76	3.53	5.36	58.86
PCM/MP4/6-31G**//MP2/6-31G**										
solvent CHCl$_3$	0.00	3.99	3.99	4.01		0.00	3.98	3.53	4.33	
solvent DMSO	0.00	4.11	3.81	4.12		0.00	4.10	3.36	4.44	
3										
MP2/6-31G**	0.30	0.00	2.02	2.50[a]	70.21[b]	0.58	0.00	0.41	3.08[a]	70.04[b]
MP4/6-31G**//MP2/6-31G**	0.52	0.00	0.63	4.26[a]	73.11[b]	0.79	0.00	−1.45	4.83[a]	72.95[b]
PCM/MP4/6-31G**//MP2/6-31G**										
solvent CHCl$_3$	0.63	0.00	−0.62	3.46[a]		0.90	0.00	−2.23	4.03[a]	
solvent DMSO	0.66	0.00	−1.05	3.55[a]		0.94	0.00	−2.65	4.13[a]	
4										
MP2/6-31G**	0.00	0.47	4.97	1.29	53.11	0.00	0.18	3.87	1.43	52.57
MP4/6-31G**//MP2/6-31G**	0.00	0.28	3.07	2.64	55.11	0.01	0.00	1.97	2.79	54.57
PCM/MP4/6-31G**//MP2/6-31G**										
solvent CHCl$_3$	0.00	1.03	2.06	2.08		0.00	0.74	0.97	2.22	
solvent DMSO	0.00	1.37	1.82	2.27		0.00	1.08	0.72	2.40	

[a] TS (b → a). [b] TS (b → c).

2. Computational and Experimental Details

2.1. Quantum Chemical Calculations. The calculations were carried out using the PC GAMESS version[19] of the GAMESS quantum chemistry package.[20] The geometries of all possible tautomeric forms of the compounds studied were located at the MP2 level using the 6-31G** basis set.[21] Selected structures were reoptimized at the same level of theory using the 6-311G**

basis set.[22] The anionic and dianionic forms of compound **3** were optimized at the MP2/6-31G** and MP2/6-31+G** levels. The transition structure for tautomeric conversion between the two most stable tautomers was located at the MP2/6-31G** and MP2/6-311G** levels. The default gradient convergence threshold (1 × 10^{-4} hartree bohr^{-1}) was used. Frequency calculations at the same levels of theory were carried out to determine

2-Substituted Indan-1,3-diones

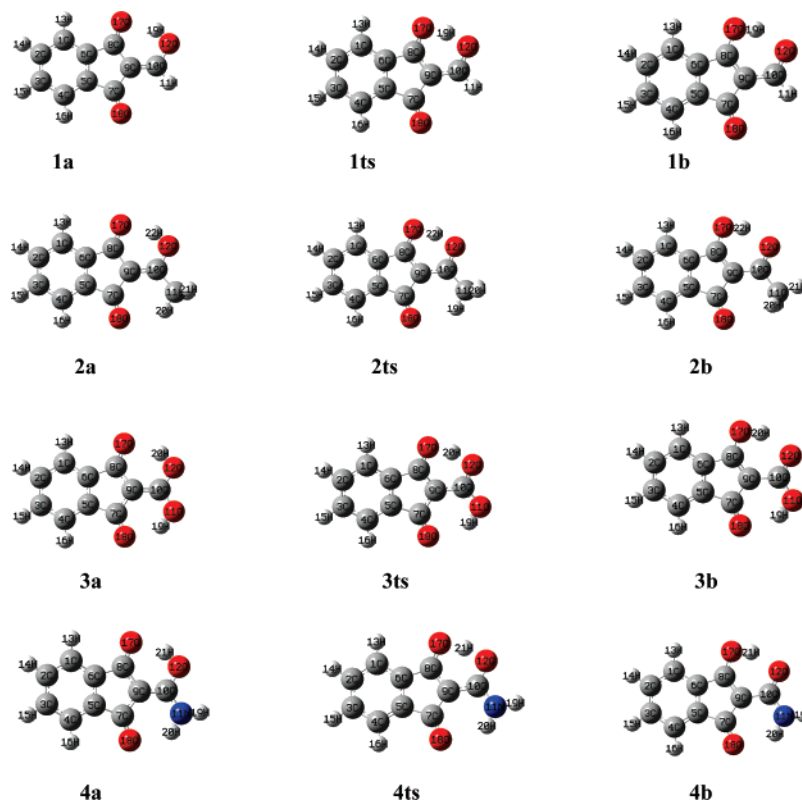*J. Phys. Chem. A, Vol. 111, No. 39, 2007* **9903**

Figure 2. Tautomeric forms **a** and **b** and **ts** of compounds **1–4**, optimized at the MP2/6-31G** level of theory.

TABLE 3: MP4/6-31G//MP2/6-31G** and MP4/6-311G**//MP2/6-311G**-Calculated Relative Enthalpies ΔH_0, Relative Gibbs Free Energies ΔG_{298}, and Activation Barriers $\Delta H_0^{\#}$ and $\Delta G_{298}^{\#}$ (in kcal mol^{-1}) for the Tautomerization Reaction a → b in 2-Substituted Indandiones[a]**

compound	isotope	ΔH_0	ΔG_{298}	$\Delta H_0^{\#}$	$\Delta G_{298}^{\#}$	k	$\nu^{\#}$
			MP4/6-31G**//MP2/6-31G** Level				
1	H	3.70	3.73	5.83	6.15	1.93×10^8	1245i
	D	3.73	3.77	6.70	7.05	4.22×10^7	928i
	T	3.74	3.79	7.07	7.45	2.15×10^7	782i
2	H	3.78	3.76	5.04	5.36	7.31×10^8	1129i
	D	3.85	3.83	5.88	6.23	1.68×10^8	844i
	T	3.88	3.87	6.24	6.62	8.71×10^7	712i
3	H	−0.52	−0.79	4.26	4.83	1.79×10^9	1242i
	D	−0.50	−0.79	5.09	5.70	4.12×10^8	921i
	T	−0.50	−0.79	5.45	6.09	2.13×10^8	774i
4	H	0.28	−0.01	2.64	2.79	5.60×10^{10}	1162i
	D	0.35	0.05	3.46	3.63	1.36×10^{10}	862i
	T	0.38	0.08	3.81	4.01	7.14×10^9	723i
			MP4/6-311G**//MP2/6-311G** Level				
1	H	3.94	4.74	5.84	6.84	6.01×10^7	1184i
	D	3.97	4.77	6.69	7.72	1.36×10^7	888i
	T	3.98	4.78	7.04	8.11	7.05×10^6	750i
2	H	4.03	5.01	5.12	6.24	1.66×10^8	1084i
	D	4.06	5.04	5.93	7.09	3.94×10^7	814i
	T	4.07	5.05	6.28	7.46	2.11×10^7	688i
3	H	−0.05	0.08	3.73	4.36	3.95×10^9	1193i
	D	−0.06	0.06	4.57	5.21	9.42×10^8	889i
	T	−0.07	0.05	4.93	5.59	4.96×10^8	748i
4	H	0.28	0.02	2.13	1.80	2.98×10^{11}	1119i
	D	0.32	0.07	2.94	2.64	7.21×10^{10}	834i
	T	0.35	0.10	3.28	3.01	3.86×10^{10}	701i

[a] Imaginary frequencies $\nu^{\#}$ are in cm^{-1}. The rate constants are in s^{-1}.

whether the optimized structures were local minima or transition states (**ts**) on the potential energy surface and to estimate thermal corrections. To obtain accurate energies, single-point calculations at the MP4/6-31G**//MP2/6-31G** and MP4/6-311G**//MP2/6-311G** levels of theory were performed. Unscaled zero-point energy (ZPE) corrections were included in the relative energy values. The theoretical IR spectra were calculated from the

harmonic force field scaled by a factor of 0.945.[23] To study isotopic effects, force field calculations for the two most stable tautomers, with the mobile protons substituted by deuterium (D) and tritium (T), were carried out.

The values of Gibbs free energies were calculated using the formula $\Delta G = \Delta H - T\Delta S$. The classical rate constants at 298.15 K were calculated using the Eyring equation, $k = (k_BT/h)$ exp-

TABLE 4: Selected MP2/6-31G**-Calculated Distances (Å) and Bond Angles (deg) for Tautomers a and b and Transition States of Compounds 1 and 2[a]

	2a			2b	2ts	1a	1b	1ts
	exptl.[7]	exptl.[9]						
Distances								
C1−C2	1.386	1.394	1.3979	1.4025	1.4007	1.3974	1.4021	1.4002
C2−C3	1.396	1.382	1.4042	1.3997	1.4012	1.4042	1.3999	1.4015
C3−C4	1.363	1.388	1.3983	1.4033	1.4017	1.3978	1.4030	1.4013
C4−C5	1.394	1.390	1.3906	1.3848	1.3867	1.3910	1.3850	1.3870
C5−C6	1.393	1.385	1.4015	1.4041	1.4048	1.4039	1.4051	1.4061
C6−C1	1.358	1.383	1.3915	1.3884	1.3894	1.3920	1.3888	1.3899
C6−C8	1.479	1.488	1.4843	1.4704	1.4728	1.4856	1.4695	1.4729
C5−C7	1.475	1.504	1.4986	1.5068	1.5084	1.4990	1.5069	1.5090
C7−C9	1.488	1.473	1.4772	1.4776	1.4714	1.4763	1.4783	1.4713
C8−C9	1.448	1.457	1.4612	1.3803	1.4070	1.4622	1.3791	1.4094
C9−C10	1.342	1.373	1.3702	1.4478	1.4120	1.3583	1.4359	1.3994
C10−C11	1.475	1.475	1.4881	1.5008	1.4951			
C7−O18	1.214	1.220	1.2320	1.2303	1.2310	1.2293	1.2284	1.2285
C8−O17	1.239	1.225	1.2462	1.3188	1.2865	1.2441	1.3205	1.2844
C10−O12	1.352	1.330	1.3332	1.2537	1.2824	1.3297	1.2495	1.2814
O12−H22(19)	1.14	0.98	0.9926	1.7063	1.2743	0.9883	1.7727	1.2601
O17−H22(19)	1.56	1.83	1.7524	1.0021	1.1620	1.8428	0.9964	1.1777
O17−O12		2.650	2.6553	2.6059	2.3924	2.7235	2.6566	2.3940
Bond Angle								
O12−H22(19)−O17			149.4	147.2	157.0	146.7	145.8	156.0

[a] Available experimental data are also given. For numbering of the atoms see Figure 2.

TABLE 5: Experimental and Calculated Chemical Shifts (ppm) of Compounds 1 and 2[a]

	experimental			GIAO HF/6-31+G*//MP2/6-31G**					
				tautomer **a**			tautomer **b**		
	CDCl3	DMSO-d6	solid state[d]	gas phase	CHCl3	DMSO	gas phase	CHCl3	DMSO
1									
C1	123.9[b]			125.8	125.9	126.0	124.9	125.9	126.2
C2	135.4[b]			133.7	135.2	135.7	132.5	133.9	134.4
C3	136.1[b]			135.6	136.7	137.1	136.0	137.3	137.7
C4	125.5[b]			125.7	125.7	125.6	125.6	125.6	125.6
C5	141.7[b]			142.6	141.9	141.7	136.9	136.4	136.3
C6	139.7[b]			139.2	138.8	138.7	134.6	133.8	133.6
C7	188.3[b]			190.3	192.0	192.6	191.2	193.0	193.6
C8	197.1[b]			201.1	201.8	202.1	194.8	196.3	196.8
C9	113.1[b]			105.6	105.7	105.7	103.9	103.8	103.8
C10	166.4[b]			172.4	173.1	173.4	195.0	195.4	195.5
O12	119.7[c]			114.6	114.3	114.2	450.6	429.2	421.7
O17	458.2[c]			431.8	416.7	411.2	125.1	127.7	128.7
O18	473.9[c]			492.6	463.9	453.8	523.7	490.1	478.7
2									
C1	122.6	122.3	125.0	125.6	125.7	125.8	124.6	125.5	125.8
C2	134.9	134.9	134.4	133.4	134.7	135.2	132.3	133.6	134.1
C3	134.0	134.9	135.0	135.1	136.3	136.7	135.4	136.6	137.0
C4	122.4	122.3	121.8	125.6	125.5	125.5	125.5	125.5	125.4
C5	138.0	139.1	138.2	142.6	142.0	141.9	137.0	136.5	136.4
C6	140.7	139.1	140.2	138.7	138.2	138.0	135.1	134.2	134.0
C7	183.6	182.4	188.6	192.1	193.4	193.9	192.6	194.0	194.5
C8	188.3	182.4	195.9	201.7	202.4	202.7	194.7	195.9	196.3
C9	108.8	108.5	109.3	102.6	102.8	102.9	103.0	102.8	102.9
C10	196.7	191.3	182.9	189.9	190.3	190.5	206.7	207.0	207.0
C11	19.1	19.4	18.3	17.5	17.6	17.6	28.1	28.2	28.3
O12	147.0[c]			135.8	135.1	134.9	432.6	416.4	410.4
O17	408.2[c]			414.3	399.6	394.4	129.0	130.4	131.0
O18	478.3[c]			490.3	468.7	460.2	524.5	497.9	487.6

[a] For numbering of the atoms, see Figure 2. [b] Reference 8. [c] Reference 10. [d] Reference 33.

$(-\Delta G^{\#}/RT)$, where k_B and h are the Boltzmann and Planck constants, respectively.

To estimate the solvent effect (chloroform (CHCl3) and dimethylsulfoxide (DMSO)) on the relative stabilities of the tautomers, the polarized continuum model (PCM)[24,25] as implemented in the Gaussian 98[26] suite of programs was applied at the MP4/6-31G**//MP2/6-31G** level.

The NMR chemical shieldings of the more stable tautomeric forms of compounds **1−4** were calculated at the HF/6-31+G* level using the GIAO[27,28] approach and the MP2/6-31G**-optimized geometry (MP2/6-31+G** for the anion and dianion of **3**). To compare to the experimental data, the calculated absolute shieldings were transformed to chemical shifts using the reference compound tetramethylsilane, Si(CH3)4, (TMS) for

2-Substituted Indan-1,3-diones

J. Phys. Chem. A, Vol. 111, No. 39, 2007 **9905**

TABLE 6: MP2/6-31G**-Calculated and Experimental IR Data in CCl₄ for Tautomer a of Compounds 1 and 2[a]

assignment	calculated	experimental
1a		
ν(OH)	3288 (103) *2393 (66)*	
ν^s(C=O)	1693 (146)	
ν^{as}(C=O)	1660 (611)	
ν(C=C)	1623 (327)	
ν(C−O)	1350 (2)	
2a		
ν(OH)	3169 (147), *2311 (100)*	3195, *2336*
ν^s(C=O)	1684 (181)	1715
ν^{as}(C=O)	1647 (509)	1658
ν(C=C)	1626 (549)	1618
ν(C−O)	1344 (39)	1290

[a] Frequencies, ν, are in cm⁻¹, and intensities (in parentheses) are in km mol⁻¹. Frequencies and intensities of deuterated compounds are in italic.

carbon and H₂O for oxygen atoms: $\delta = \delta_{calc}(ref) - \delta_{calc}$. Both $\delta_{calc}(ref)$ and δ_{calc} were evaluated at the same computational level.

The inclusion of the solvent as a dielectric (polarizable continuum model) in GIAO NMR calculations was used to estimate the effect of the medium (CHCl₃ and DMSO) on the chemical shifts of the more stable tautomers of the studied compounds. All NMR calculations were carried out using Gaussian 03.[29]

The MP2/6-31G**-optimized geometries for the tautomeric forms and MP2/6-31+G** ones for the anion and dianion of **3** were used for the vertical transition energy calculations in time-dependent density functional theory (TDDFT).[30] The B3LYP functional[31] and the aug-cc-pVDZ basis set[32] were used in the TDDFT calculations.

2.2. Experimental Details. 2-Acetyl-indan-1,3-dione **2** was synthesized according to a previously published procedure,[33]

2-carboxy-indan-1,3-dione **3** according to ref 18, and 2-carboxyamide-indan-1,3-dione **4** according to ref 14.

NMR spectra were recorded on a Bruker DRX-250 spectrometer, operating at 250.13 MHz for ¹H and 62.9 MHz for ¹³C, using a 5 mm dual probe head. The chemical shifts were referenced to TMS in CDCl₃ and to the solvent signal in DMSO-d_6. The measurements were carried out at ambient temperature (ca. 300 K) in solvents CDCl₃ and DMSO-d_6. Sample concentrations of 0.01−0.05 M for ¹H and saturated solutions for ¹³C NMR spectra were used.

The deuterium exchange of the mobile protons of 2-(hydroxyaminomethylidene)-indan-1,3-dione (**2**) was achieved by dissolving 20 mg of the compound in 1 mL of chloroform and stirring with 0.3 mL of D₂O. The organic phase was separated and treated with another portion of 0.3 mL of D₂O. The procedure was repeated to complete deuterium exchange of the mobile protons, and the process was monitored by ¹H NMR. The 2-carboxy-indan-1,3-dione (**3**) was deuterated by dissolving 3 mg of the compound in 5 mL of D₂O.

IR spectra of **2−4** were recorded with the IFS 113v and "Tensor 27" Bruker FTIR spectrometers in the spectral region of 4000−400 cm⁻¹. Solid-state spectra of **2−4** were measured in a KBr pellet. IR spectra of saturated solutions of **2** and **4** in CCl₄ were measured in a 1 mm KBr liquid cell while those of the saturated solutions of **3** and **4** in CH₂Cl₂ and CH₃CN were recorded using 0.6 mm KBr liquid cell. Saturated solutions of the deuterated compound **2** in CCl₄ were also studied.

The absorption spectra of compounds **2−4** were recorded on a Specord M40 UV−vis spectrophotometer in ethanol. Solutions with concentrations of 1 × 10⁻⁴ M L⁻¹ were used.

The mass spectrometry analysis of **3** was carried out on a 70 eV Hewlett-Packard HP-5973 electron impact mass spectrometer. The melting point of compound **3** was measured on a BOETIUS (type PHMK05) apparatus.
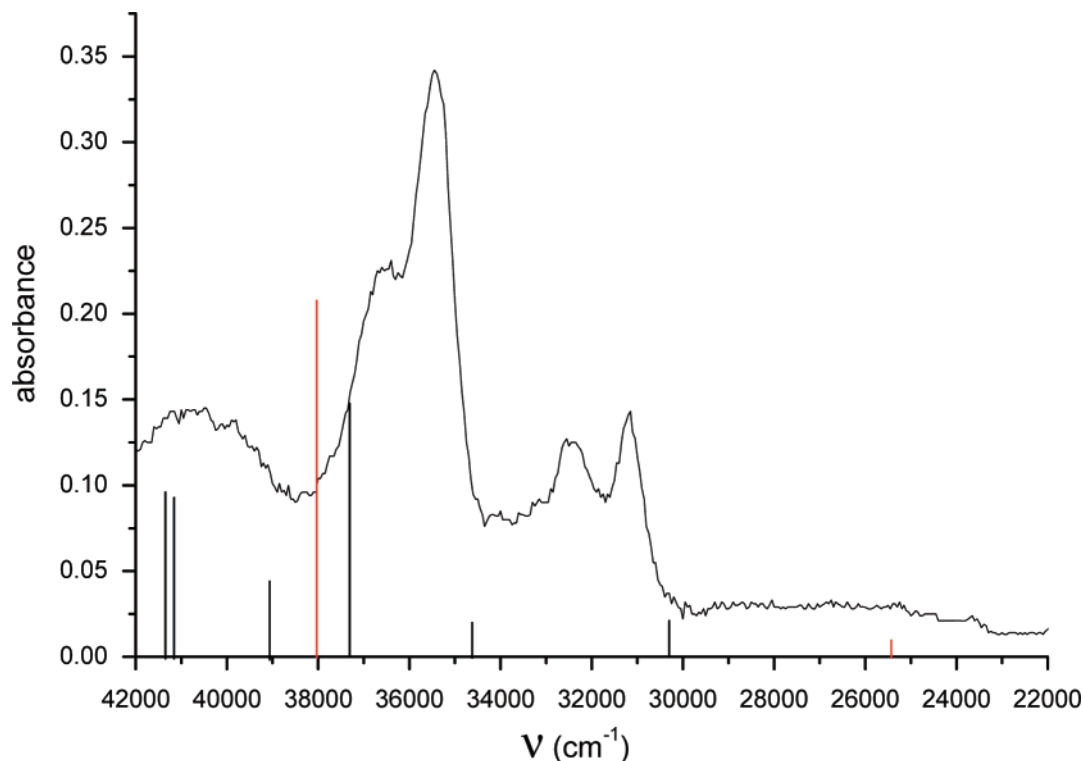

Figure 3. UV absorption spectrum of 2-acetylindan-1,3-dione in ethanol. Optical density (OD) is in arbitrary units, and wavelength is in cm⁻¹. TDDFT B3LYP/aug-cc-pVDZ-calculated $\pi-\pi^*$ electron transitions for tautomer **b** (red line) and tautomer **a** (black line).

TABLE 7: Experimental and GIAO ^{13}C Chemical Shifts (ppm) Calculated at the HF/6-31+G* Level of Theory of Compound 4

| | experimental | | GIAO HF/6-31+G*//MP2/6-31G** | | | | | | a/b^a | | a/b^b | |
| | | | tautomer **a** | | | tautomer **b** | | | | | | |
	CDCl$_3$	DMSO-d_6	gas phase	CHCl$_3$	DMSO	gas phase	CHCl$_3$	DMSO	gas phase	PCM	gas phase	PCM
C1	121.1	120.9	125.0	125.0	125.0	124.1	124.8	125.1	124.8	125.0	124.9	125.0
C2	132.8	133.1	133.0	134.0	134.4	132.8	134.0	134.5	132.9	134.0	133.0	134.4
C3	132.8	133.1	133.9	134.9	135.3	134.3	135.5	135.9	134.0	135.0	133.9	135.4
C4	121.1	120.9	124.9	124.8	124.8	125.5	125.6	125.6	125.0	125.0	125.0	124.9
C5	138.5	138.2	141.3	140.7	140.5	136.3	135.7	135.5	140.2	139.6	140.6	139.8
C6	138.5	138.2	139.7	139.1	138.9	136.2	135.3	135.1	139.0	138.3	139.2	138.4
C7	192.5	191.1	194.9	195.8	196.1	195.2	196.3	196.7	195.0	195.9	195.0	196.2
C8	192.5	191.1	200.0	200.7	200.9	192.9	193.8	194.2	198.4	199.2	199.0	200.0
C9	95.1	92.2	85.9	86.1	86.2	96.1	95.6	95.5	88.2	88.2	87.3	87.5
C10	168.7	167.5	171.4	171.6	171.7	172.4	172.8	172.8	171.6	171.9	171.5	171.9

^{a} **a/b** = 77.7:22.3% (solvent CHCl$_3$). ^{b} **a/b** = 86.1:13.9% (solvent DMSO).

TABLE 8: MP2/6-31G-Calculated and Experimental IR Data for Tautomers a and b of Compound 4^a**

| | | experimental | | |
assignment	calculated	CCl$_4$	CH$_2$Cl$_2$	CH$_3$CN
		4a		
ν^{as}(NH$_2$)	3609 (180)	3500 s		3550 s *
ν^s(NH$_2$)	3390 (95)	3317 w		
ν(OH)	3104 (5)	3617 w	3470 s *	3620 s *
ν^s(C=O)	1682 (965)	1696 vs	1695 vs	1697 vs
ν^{as}(C=O)	1640 (600)	1656 vs	1658 vs	1632 vs
ν(C−O)	1463 (58)	1413 w *		
		4b		
ν^{as}(NH$_2$)	3578 (126)	3459 s		3550 s *
ν^s(NH$_2$)	3418 (71)	3340 s		
ν(OH)	3013 (396)		3470 s *	3620 s *
ν^s(C=O)	1676 (526)	1696 vs	1670 sh	1668 sh
ν^{as}(C=O)	1661 (40)		1635 s	1632 s
ν(C−O)	1463 (30)	1413 w *		

^{a} Frequencies, ν, are in cm^{-1}, and intensities (in parentheses) are in km mol^{-1}.
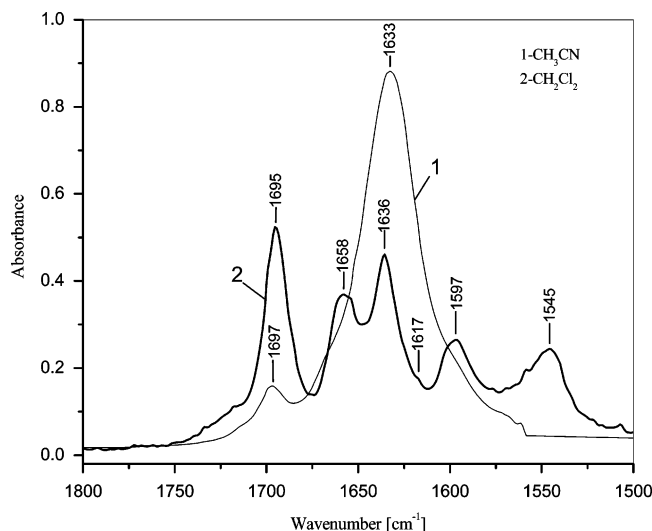
Figure 4. IR spectrum of 2-carboxyamide-indan-1,3-dione in CH$_3$CN and CH$_2$Cl$_2$.

3. Results and Discussion

3.1. Gas-Phase Results: Relative Stabilities. All possible tautomers of compounds **1**−**4**, presented in Figure 1, are considered in our study. Geometry optimizations were carried out at the MP2/6-31G** level of theory for all species. The relative energies of three tautomeric forms for **1** and **3** and five tautomers for **2** and **4** are presented in Table 1. The calculations show that for all compounds tautomer **a** has the lowest energy.

For compounds **1** and **2**, the energy difference between tautomers **a** and **b** is in the range of 3.75−4.11 kcal mol^{-1}, while for compound **4** it is smaller, 0.93 kcal mol^{-1}. In the case of compound **3** this difference is very small, only 0.14 kcal mol^{-1}. Tautomer **c** is also near in energy to the most stable tautomeric form of compound **3**.

Tautomeric forms **a** and **b** of compounds **1**−**4** were reoptimized at the MP2/6-311G** level. The energy differences between tautomers **a** and **b** for compounds **1** and **2** decrease in comparison with the results obtained at the MP2/6-31G** level, while for compounds **3** and **4** there are no changes.

To obtain more accurate energies, single-point calculations at the MP4/6-31G**//MP2/6-31G** and MP4/6-311G**//MP2/6-311G** levels of theory were performed. The energy differences between tautomers **a** and **b** for compounds **1** and **2** increase in comparison with the results obtained at the MP2 level. The opposite tendency is observed for compounds **3** and **4**; tautomer **3b** becomes even more stable. The energy differences between the most stable tautomer and tautomer **c** decrease by about 2 kcal mol^{-1} in comparison to the results obtained at the MP2 level. The energy difference between tautomers **3b** and **3c** becomes small − 0.58 kcal mol^{-1}. For compounds **2** and **4** the energy differences between the most stable tautomer and tautomers **d** and **e** are large − in the range of 13.65−28.77 kcal mol^{-1}.

3.2. Thermodynamics. The differences in relative energies of the tautomers suggest that, in the gas phase, the molecules should exist as a mixture of tautomers. However, the differences in the relative energies correspond to the relative order of the minima on the potential energy surface. To predict the order of relative stabilities, one should include thermal and entropy corrections. To investigate the influence of these parameters, we have calculated the order of relative stabilities. The results are collected in Table 2.

Inclusion of ZPE correction in the relative stabilities at the MP2/6-31G** and MP4/6-31G**//MP2/6-31G** levels decreases the energy differences between tautomers **a** and **b** and tautomers **a** and **c** for compounds **1**, **2**, and **4** (Table 2). However, at the MP4/6-31G**//MP2/6-31G** level the enthalpy differences, ΔH_0, between tautomers **b** and **c** of compounds **1** and **2** are small, 0.18 and 0.19 kcal mol^{-1}, respectively. Calculations at the MP2/6-31G** level predict tautomer **3b** as the most stable, and the difference between tautomers **3b** and **3a** is 0.30 kcal mol^{-1}, while the enthalpy difference between tautomers **3b** and **3c** is 2.02 kcal mol^{-1}. However, at the MP4/6-31G**//MP2/6-31G** level the enthalpy difference between tautomers **3b** and **3c** decreases to 0.63 kcal mol^{-1}, and the difference between **a** and **c** is found to be only 0.11 kcal mol^{-1}.

2-Substituted Indan-1,3-diones

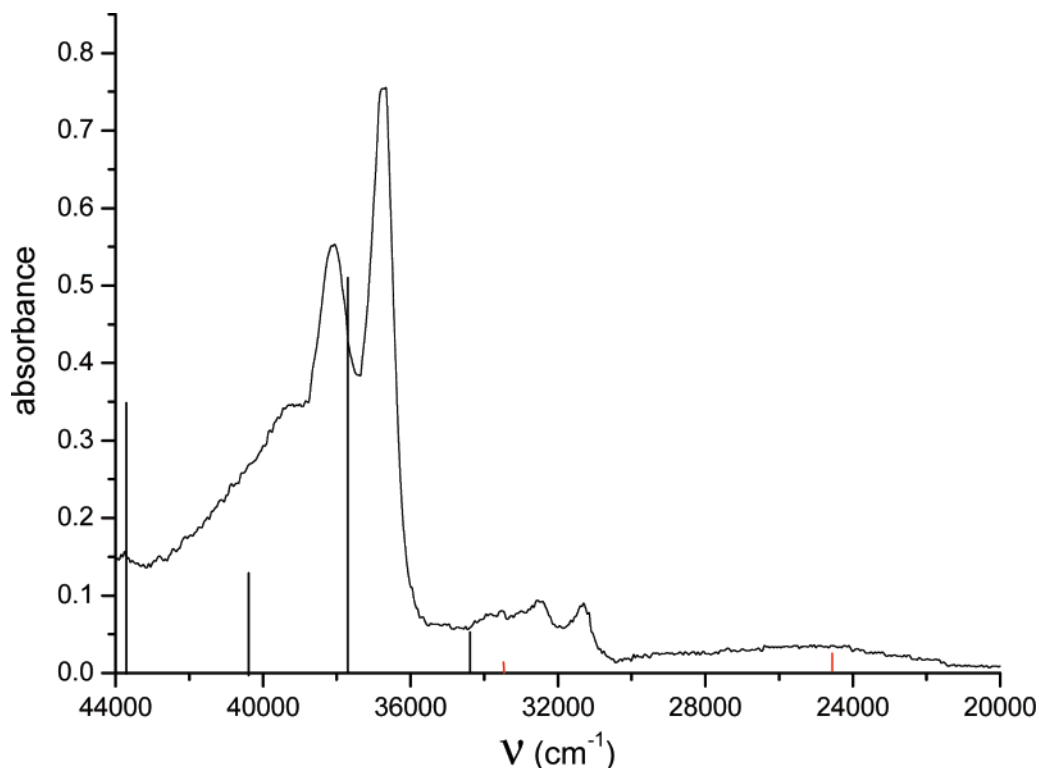*J. Phys. Chem. A, Vol. 111, No. 39, 2007* **9907**

Figure 5. UV absorption spectrum of 2-carboxyamide-indan-1,3-dione in ethanol. Optical density (OD) is in arbitrary units, and wavelength is in cm^{-1}. TDDFT B3LYP/aug-cc-pVDZ-calculated $\pi-\pi^*$ electron transitions for tautomer **b** (red line) and tautomer **a** (black line).

The gas-phase-calculated Gibbs free energy differences of tautomers **a**, **b**, and **c** obtained at the MP2/6-31G** and MP4/6-31G**//MP2/6-31G** levels are presented in Table 2.

For all compounds, the effect of the frequency-dependent corrections is stronger on the tautomeric forms **c** than on **a** and **b**. However, at the MP4/6-31G**//MP2/6-31G** level tautomers **c** of compounds **1** and **2** become preferred to **b**. For compound **3** the preferred tautomer is **c**. The energy differences between tautomers **b** (next in energy) and **a** are small, 0.79 kcal mol^{-1}. The situation for compound **4** is complicated; tautomers **a** and **b** are predicted to be almost isoenergetic (0.18 kcal mol^{-1} at the MP2 level and 0.01 kcal mol^{-1} at the MP4 level).

The PCM-calculated relative stabilities in solvents CHCl$_3$ and DMSO for tautomers **a**, **b**, and **c** obtained at the MP2/6-31G** and MP4/6-31G**//MP2/6-31G** levels are also presented in Table 2. For compounds **1** and **2** including the CHCl$_3$ solvent effect does not influence the differences between **a** and **c** tautomers, while the differences between **a** and **b** increase by 0.05 kcal mol^{-1} for **1** and 0.22 kcal mol^{-1} for **2**. As a result tautomer **c** becomes more stable than **b**. For compound **3** the situation is different; tautomer **c** is most influenced by consideration of the solvent, and the difference between the preferred tautomer **c** and the next in energy tautomer **b** increases by 0.78 kcal mol^{-1} in comparison to the MP4/6-31G**//MP2/6-31G** result in the gas phase. For compound **4** including the solvent effect makes tautomer **a** the most stable (next in energy is tautomer **b**) and decreases the energy differences between **a** and **c**.

For compounds **1**, **2**, and **4** taking into account the solvent effect (DMSO) decreases the energy differences between the most stable tautomer (**a** or **b**) and tautomer **c**, while the differences between **a** and **b** are less influenced. For compound **3** the difference (ΔG_{298}) between the preferred tautomer **c** and the next in energy tautomer **b** increases by 1.2 kcal mol^{-1} in comparison to the MP4/6-31G**//MP2/6-31G** result in the gas phase.

The intramolecular proton-transfer barriers between tautomers **a** and **b** and tautomers **a** and **c** for compounds **1**−**4** were calculated at the MP4/6-31G**//MP2/6-31G** level of theory (Table 2). The MP4/6-31G**//MP2/6-31G**-calculated values of the proton-transfer barriers of tautomerization **a** → **b** (**b** → **a** for compound **3**) are in the range of 2.79−6.15 kcal mol^{-1}. The inclusion of solvent (CHCl$_3$ and DMSO) as a dielectric decreases the barrier heights for all compounds studied, and the decrease is stronger for CHCl$_3$. The values of the proton-transfer barriers for compound **4**, 2.22 in CHCl$_3$ and 2.40 kcal mol^{-1} in DMSO, indicate an extremely fast proton-transfer process.

The values of the proton-transfer barriers of tautomerization **a** → **c** are quite large (in the range of 54.57−72.95 kcal mol^{-1}), and tautomerization should not occur. The absence of the signal at about 55−60 ppm for C9(H) carbon atoms for **1**−**4** and DEPT-135 experiments in CDCl$_3$ and DMSO-d_6 confirm the exclusion of tautomer **c**.[8,15,33]

3.3. Influence of the Isotopic Substitution on the Thermodynamics and Kinetics of Tautomerization. Calculations at the MP4/6-31G**//MP2/6-31G** and MP4/6-311G**//MP2/6-311G** levels of theory were performed to investigate the influence of isotopic substitution of the mobile hydrogen atoms in compounds **1**−**4** on the thermodynamics and kinetics of the tautomerization reaction **a** → **b** (Table 3 and Figure 2).

The calculations at the MP4/6-311G**//MP2/6-311G** level for compounds **1** and **2** show weak increases of $\Delta H_0^{\#}$ in comparison to the MP4/6-31G**//MP2/6-31G**-calculated ones, while $\Delta G_{298}^{\#}$ increases by 0.69 kcal mol^{-1} for **1** and 0.88 kcal mol^{-1} for **2**. The situation is different for compounds **3** and **4**; the calculated barriers of activation $\Delta G_{298}^{\#}$ are low at the MP4/6-31G**//MP2/6-31G** level (4.83 kcal mol^{-1} for **3** and 2.79 kcal mol^{-1} for **4**) and decrease at the MP4/6-311G**//MP2/6-311G** level of theory (4.36 kcal mol^{-1} for **3** and 1.80 kcal mol^{-1} for **4**).

TABLE 9: Selected MP2/6-31G**-Calculated Distances (Å) and Bond Angles (deg) for Tautomers a, b, and c, Anion, and Dianion of Compound 3[a]

	3a	3b	3c	an1	an2	dianion
			Distances			
C1−C2	1.3999	1.4040	1.3946	1.4041 (1.4065)	1.4030 (1.4052)	1.4122 (1.4141)
C2−C3	1.4021	1.3984	1.4071	1.3998 (1.4026)	1.4011 (1.4038)	1.3963 (1.4000)
C3−C4	1.3999	1.4042	1.3946	1.4039 (1.4062)	1.4028 (1.4053)	1.4122 (1.4142)
C4−C5	1.3892	1.3842	1.3950	1.3871 (1.3898)	1.3876 (1.3904)	1.3855 (1.3889)
C5−C6	1.4078	1.4074	1.3983	1.3966 (1.3989)	1.3936 (1.3961)	1.3977 (1.4006)
C6−C1	1.3892	1.3866	1.3951	1.3858 (1.3885)	1.3878 (1.3903)	1.3855 (1.3889)
C6−C8	1.4953	1.4747	1.4821	1.5183 (1.5173)	1.5138 (1.5123)	1.5192 (1.5165)
C5−C7	1.4953	1.5016	1.4820	1.5021 (1.5008)	1.5132 (1.5120)	1.5190 (1.5164)
C7−C9	1.4431	1.4631	1.5403	1.4218 (1.4250)	1.4469 (1.4482)	1.4271 (1.4276)
C8−C9	1.4431	1.3710	1.5404	1.4481 (1.4508)	1.4458 (1.4492)	1.4271 (1.4277)
C9−C10	1.3780	1.4530	1.5074	1.4599 (1.4609)	1.4370 (1.4386)	1.5365 (1.5252)
C10−O11	1.3167	1.3425	1.3509	1.3723 (1.3754)	1.3871 (1.3882)	1.2670 (1.2734)
C7−O18	1.2448	1.2371	1.2234	1.2641 (1.2680)	1.2429 (1.2484)	1.2608 (1.2660)
C8−O17	1.2448	1.3206	1.2234	1.2401 (1.2439)	1.2440 (1.2471)	1.2608 (1.2660)
C10−O12	1.3167	1.2349	1.2187	1.2257 (1.2289)	1.2339 (1.2376)	1.2670 (1.2734)
O12−H20	0.9901	1.8436				
O17−H20	1.8997	0.9935				
O11−H19	0.9901	0.9791	0.9726	0.9886 (0.9914)	0.9706 (0.9721)	
O17−O12	2.7842	2.7138		3.1450 (3.1395)	3.0238 (3.0197)	3.6428 (3.7175)
O18−O11	2.7842	2.8913		2.6700 (2.6678)	2.8482 (2.8475)	3.6406 (3.7177)
C9−H20			1.0903			
			Torsion Angle			
O12−C10−C9−C8	6.4	0.0	0.3 (7.1)	0.1 (1.8)	81.7 (88.3)	
O11−C10−C9−C8	−174.3	180.0	179.9 (−173.8)	−179.9 (−178.8)	−98.3 (−91.6)	

[a] For numbering of the atoms, see Figure 2. MP2/6-31+G**-calculated distances are given in parentheses.

The substitution of the mobile protons attached to oxygen and nitrogen atoms with deuterium and tritium leads to slight increases (0.02−0.11 kcal mol^{-1}) in $\Delta H_0^\#$ and ΔG_{298} in comparison to the unsubstituted compounds with the exception of compound **3**, where there is no change at the MP4/6-31G**// MP2/6-31G** level and a slight decrease (from 0.08 to 0.05 kcal mol^{-1}) at the MP4/6-311G**//MP2/6-311G** level.

The activation enthalpies $\Delta H_0^\#$ and free activation energies $\Delta G_{298}^\#$ increase faster upon substitution. In all cases the free activation energies $\Delta G_{298}^\#$ have higher values than the activation enthalpies $\Delta H_0^\#$ with the exception of compound **4**. However, the predicted values for **4** are low, and the process of proton transfer should be fast on the NMR time scale. The rate constants of the tautomerization reaction a → b calculated by the Eyring equation are found to be on the order of $1 \times 10^6 - 1 \times 10^9$ s^{-1} for compounds **1**, **2**, and **3**. For compound **4** they are on the order of $1 \times 10^9 - 1 \times 10^{11}$ s^{-1}, and this suggests that the proton-transfer reaction is extremely fast.

3.4. 2-Formyl-indan-1,3-dione and 2-Acetyl-indan-1,3-dione. The MP2/6-31G**-calculated bond lengths for tautomers **a** and **b** of **2** and available X-ray data[7,9] are summarized in Table 4. There is reasonable agreement between the results obtained by ab initio calculations and crystallographic data for compound **2**. According to Antipin et al.[9] the experimental O12⋯O17 distance in **2** (at −120 °C) is 2.650 Å, indicating the presence of an O−H⋯O intramolecular hydrogen bond. The MP2/6-31G** calculations predict this distance to be 2.655 Å.

The ^{13}C NMR data obtained at room temperature for **2** in the solid state and in CHCl$_3$ and DMSO solution are listed in Table 5. A significant downfield shift of the resonance peak of the carbonyl carbon C8 compared to solution ($\Delta = \delta_{solution} - \delta_{solid} = -7.6$ and −13.5 ppm for CHCl$_3$ and DMSO, respectively) and an upfield shift of the hydroxyl substituted carbon C10 ($\Delta = 13.8$ and 8.4 ppm for CHCl$_3$ and DMSO, respectively) indicate the existence of a hydrogen-bonded cycle, in agreement with X-ray diffraction results. The formation of the O12−H⋯O17 hydrogen bond stiffens the molecule and in-creases its asymmetry. Therefore, in the cross-polarization magic-angle spinning spectrum of **2**, separate resonances for particular carbons are observed (Table 5); the signals of C1 and C4 are separated by 3.2 ppm, the signals of C5 and C6 by 2.0 ppm, and those of C2 and C3 by 0.6 ppm.

The carbon and oxygen chemical shifts of tautomers **a** and **b** of compounds **1** and **2** are presented in Table 5. As mentioned above, because of the experimentally proven absence of tautomer **c** in solution, the chemical shifts of tautomers **c** are not presented. There is good agreement between the experimental ^{17}O and calculated chemical shifts without the inclusion of solvent effects (CHCl$_3$) for tautomers **a** of compounds **1** and **2** ($\Delta\delta = -4.3$ ppm for **1a** and 2.3 ppm for **2a**) and unreliable prediction of chemical shifts ($\Delta\delta = -19.0$ ppm for **1a** and −10.0 ppm for **2a**) when the solvent effect is taken into account.

Taking into account the solvent effect for the carbon chemical shifts of tautomers **a** and **b** of compounds **1** and **2** actually worsens the agreement with the ^{13}C experimental data.

There is good agreement between the experimental and the calculated chemical shifts of tautomers **a**. For compound **1** the most noticeable disagreements between calculated and experimental ^{13}C chemical shifts concerns C9 ($\Delta\delta = -7.5$ ppm), C10 ($\Delta\delta = 6.0$ ppm) and C8 ($\Delta\delta = 4.0$ ppm), while the values for C3, C4, C5, and C6 are more accurate ($\Delta\delta < 1.0$ ppm). The average deviation between the calculated and the experimental ^{13}C NMR spectrum is 0.5 ppm for **1a**.

For compound **2** the calculated carbon chemical shifts are close to the experimental results in the solid state and in CDCl$_3$ solution. In both cases the average deviations between the calculated and the experimental ^{13}C NMR spectra are 1.4 ppm for **2a**. The noticeable disagreements between calculated and experimental chemical shifts in CDCl$_3$ solution concern C8 ($\Delta\delta = 13.4$ ppm), C7 ($\Delta\delta = 8.5$ ppm), C9 ($\Delta\delta = -6.2$ ppm), and C10 ($\Delta\delta = -6.8$ ppm). There is relatively good agreement between the experimental solid-state and the calculated chemical shift for C8 ($\Delta\delta = 5.8$ ppm).

2-Substituted Indan-1,3-diones

J. Phys. Chem. A, Vol. 111, No. 39, 2007 **9909**

TABLE 10: Experimental Data and Calculated Chemical Shifts (ppm) of Tautomers a, b, and c, Anion, and Dianion of Compound 3[a]

| | | GIAO HF/6-31+G*//MP2/6-31G** | | | | | | | | | |
| | | tautomer **a** | | tautomer **b** | | tautomer **c** | | **anion** | | **dianion** | |
	experimental (DMSO)	gas phase	DMSO	gas phase	DMSO	gas phase	DMSO	gas phase	DMSO	gas phase	DMSO
C1	120.1	125.7	125.9	125.0	126.4	126.7	126.9	122.2 (122.5)	123.1 (123.5)	116.5	121.0
C2	132.3	134.5	136.1	133.6	135.3	135.8	138.1	127.5 (128.6)	132.3 (133.6)	122.0	130.2
C3	132.3	134.5	136.1	135.3	137.1	135.8	138.1	127.4 (127.6)	132.4 (132.6)	122.0	130.2
C4	120.1	125.7	125.9	126.1	126.3	126.7	126.9	122.3 (122.0)	123.3 (123.7)	116.5	121.0
C5	138.6	140.3	139.6	135.6	134.9	144.2	143.6	145.3 (143.9)	141.8 (139.9)	154.0	144.7
C6	138.6	140.3	139.6	135.8	134.5	144.2	143.6	145.2 (145.0)	141.8 (141.6)	154.0	144.6
C7	192.2	197.9	199.0	196.9	198.3	197.0	199.2	193.4 (199.0)	196.4 (202.0)	190.0	194.2
C8	192.2	197.9	199.0	192.6	194.8	197.0	199.2	194.7 (192.9)	198.1 (196.4)	190.1	194.3
C9	97.7	86.9	87.3	94.7	93.7	55.4	55.7	90.6 (94.2)	89.4 (91.5)	121.5	112.2
C10	166.0	176.3	175.9	171.4	172.1	172.3	174.1	170.3 (168.8)	171.5 (170.7)	180.5	183.9
O11		125.7	124.0	153.8	150.5	177.5	180.7	165.0 (148.0)	162.3 (148.1)	305.1	292.2
O12		125.7	124.0	313.2	292.3	381.1	365.3	307.6 (334.3)	286.8 (298.7)	305.1	292.2
O17		411.9	391.6	125.8	128.9	569.7	532.0	434.6 (455.1)	397.5 (413.1)	333.0	311.4
O18		411.9	391.6	479.5	447.3	569.5	532.0	418.3 (322.5)	395.3 (320.1)	332.9	311.2

[a] The calculated chemical shifts of the anionic form with an intramolecular hydrogen bond are given in parentheses. For numbering of the atoms, see Figure 2.
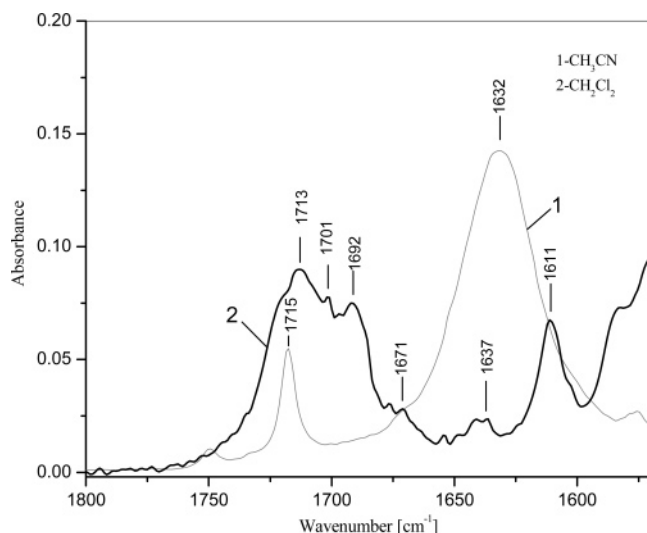
Figure 6. IR spectrum of 2-carboxy-indan-1,3-dione in CH_3CN and CH_2Cl_2.

TABLE 11: MP2/6-31G**-Calculated and Experimental IR Data for Tautomer b and the Anion of Compound 3[a]

| | | | experimental | |
assignment	calculated		CH_2Cl_2	CH_3CN
	3b	**3b1**		
ν(O11−H19)	3435 (167)	3566 (122)		3540
ν(O17−H20)	3176 (263)	3186 (272)		
ν(C10=O12)	1706 (366)	1685 (181)	1701	
ν(C7=O18)	1662 (179)	1665 (338)	1692	
	an1	**an2**		
ν(O11−H19)	3191 (277)	3568 (28)		3640
ν(C10=O12)	1735 (599)	1704 (595)	1713	1715
ν^s(C=O)	1650 (74)	1654 (219)	1671	1671
ν^{as}(C=O)	1605 (341)	1627 (468)	1637	1632

[a] Frequencies, ν, are in cm^{-1}, and intensities (in parentheses) are in km mol^{-1}.

Selected MP2/6-31G**-calculated and available experimental vibrational frequencies of tautomers **a** of compounds **1** and **2** are given in Table 6. Our assignments for the ab initio calculated frequencies are based upon the analysis of the corresponding vibrational eigenvectors.

The calculated stretching modes of the C=O bonds of both compounds are in the interval of 1720−1650 cm^{-1}, which is commonly observed for indandione and its derivatives.[34,35] The ν(C=C) mode is observed at 1618 cm^{-1}. The ν(OH) frequency mode is found at 3195 cm^{-1}, while after deuterium exchange ν(OD) appears at 2336 cm^{-1}. There is a good agreement between the calculated and the experimental data for compound **2** (Table 6).

The UV absorption spectrum of **2** consists of three intensive bands in the 42 000−30 000 cm^{-1} region. TDDFT B3LYP/aug-cc-pVDZ calculations were performed to predict the absorption maxima of compound **2**. For tautomer **a** absorption maxima are predicted at 37 376, 41 169, and 41 701 cm^{-1} and are found to be in relatively good agreement with the corresponding experimental data (Figure 3). For tautomer **2b**, an intensive absorption maximum is calculated at 38 007 cm^{-1}, and a low intensive absorption maximum is calculated at 25 425 cm^{-1}. Because of a very low concentration of tautomer **2b**, it could not be detected.

3.5. 2-Carboxyamide-indan-1,3-dione. As we proved in ref 15, the tautomeric forms **4a** and **4b** coexist in the gas phase and in solution, with fast intramolecular proton transfer between them. Because of the difficulty of direct comparison between the experimental and the calculated chemical shift values, average carbon chemical shifts (calculated on the basis of the IPCM[36] (static isodensity surface polarized continuum model) relative populations of tautomers **a** and **b**) in $CHCl_3$ and DMSO were calculated and compared to the experimentally observed values. The average differences between the average chemical shifts obtained at MP2/6-31G**-optimized geometries and the corresponding experimentally observed values showed relatively low average deviations ($\Delta\delta$). The experimental results were consistent with a mixture of tautomers **4a** and **4b** in solution. Herein we perform a similar scheme using PCM relative populations of tautomers **4a** and **4b** in $CHCl_3$ and DMSO and combine NMR calculations in solvent (PCM) with averaged[15] (on the basis of populations) carbon chemical shifts. The carbon chemical shifts of **4a** and **4b** calculated at the Hartree−Fock (HF) level without taking into account the solvent effect are closer to the experimental data than those calculated in solvent (Table 7). The gas-phase results for both tautomers are closer to the experimental results in $CDCl_3$ solution; the average deviations ($\Delta\delta$) are 1.6 ppm for **4a** and 1.2 ppm for **4b**. The
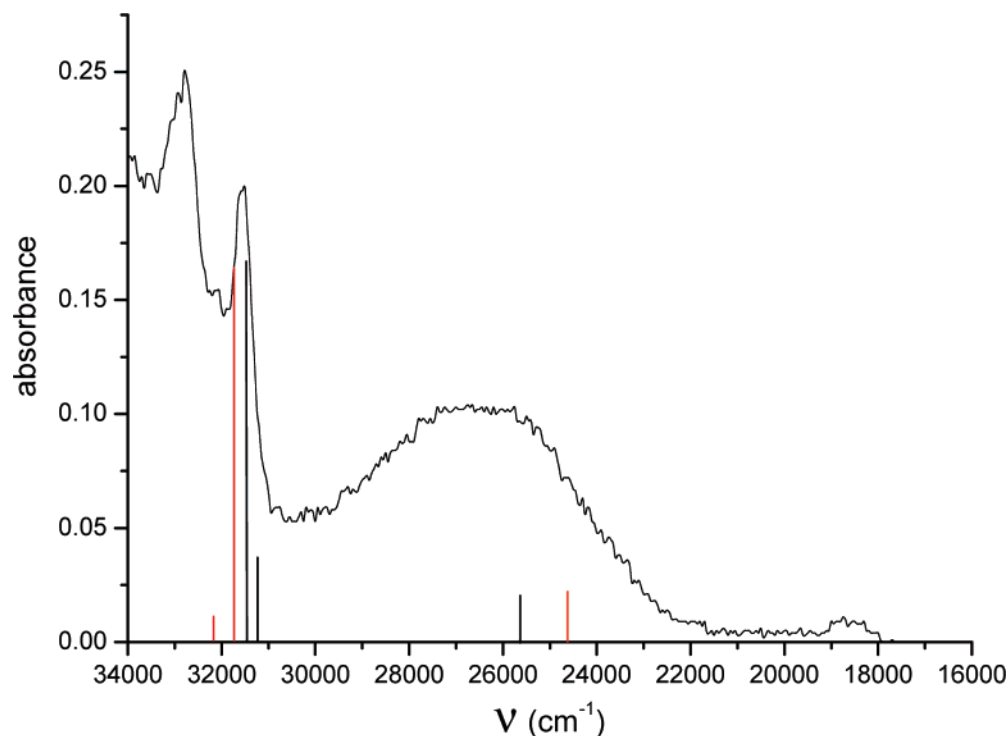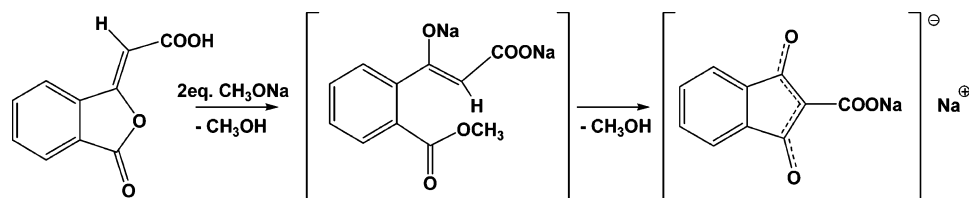
Figure 7. UV absorption spectrum of 2-carboxy-indan-1,3-dione in ethanol. Optical density (OD) is in arbitrary units, and wavelength is in cm^{-1}. TDDFT B3LYP/aug-cc-pVDZ-calculated $\pi-\pi^*$ electron transitions for the anionic forms: **an1** (black line) and **an2** (red line).

SCHEME 1

average deviations relative to DMSO experimental results are 2.4 and 2.0 ppm for **4a** and **4b**, respectively. It can be seen that the use of this scheme leads to no improvement in the calculated values of the chemical shifts of these tautomers; the average deviations ($\Delta\delta$) stay in the same range, 1.5−1.8 ppm for CHCl$_3$ and 2.3−2.7 ppm for DMSO.

In the present work the ab initio and experimental IR spectra of 2-(hydroxyaminomethylidene)-indan-1,3-dione (**4a**) and 2-carboamide-1-hydroxy-3-oxo-indan (**4b**) are compared in an attempt to prove the existence of both tautomers in solution.

The vibrational spectra of tautomers **4a** and **4b** are computed at the MP2/6-31G** level. Selected calculated and experimental (in CCl$_4$, CH$_2$Cl$_2$, and CH$_3$CN) vibrational frequencies of the tautomers are presented in Table 8. The stretching modes of the C=O bonds of tautomers **4a** and **4b** are complex since there are mixed vibrations. The ν^{as}(C=O) vibrations are calculated to be 1640 and 1661 cm^{-1} for tautomers **4a** and **4b**, respectively, while ν^s(C=O) of both tautomers in CCl$_4$ are close, 1682 cm^{-1} (**4a**) and 1676 cm^{-1} (**4b**). The observed in CH$_2$Cl$_2$ frequency modes at 1695 cm^{-1} (ν^s(C=O)) and 1658 cm^{-1} (ν^{as}(C=O)) show the presence of tautomer **4a**. The carbonyl frequency modes of **4b** are found at 1670 cm^{-1} (shoulder) and 1635 cm^{-1}. The change in the solvent polarity leads to a change in the band intensity of the corresponding carbonyl modes (Figure 4), which strongly overlap each other.

The ν(OH) frequency modes observed above 3500 cm^{-1} in solvents CCl$_4$ and CH$_3$CN correspond to a hydroxyl group uninvolved in a hydrogen bond, while those at 3470 cm^{-1} in CH$_2$-

Cl$_2$ belong to a hydrogen-bonded hydroxyl group. The predicted value of ν(OH) frequency modes, 3104 cm^{-1}, is very low.

TDDFT B3LYP/aug-cc-pVDZ calculations were performed to predict the absorption maxima of compound **4**. For tautomer **a** absorption maxima are predicted at 34 540, 37 648, and 40 292 cm^{-1}, and they are in relatively good agreement with the experimental data (Figure 5). For tautomer **b** a low-intensive long-wavelength absorption maximum is calculated at 24 631 cm^{-1}. The experimentally observed absorption band at about 25 500 cm^{-1} proves the existence of tautomer **b** in solution.

3.6. 2-Carboxy-indan-1,3-dione. 2-Carboxy-indan-1,3-dione, **3**, was synthesized by Perkin condensation of phthalic anhydride with acetic anhydride and potassium acetate followed by isomerization of the phthalidene acetic acid with sodium methoxide (Scheme 1) and subsequent hydrolysis of the sodium salt with HCl leading to **3**. Upon heating of **3**, carbon dioxide was released and indan-1,3-dione was obtained.[17,18]

Compound **3** synthesized according to ref 18 is a crystalline powder (mp 295−302 °C (dec)) of ochre color. The electron impact mass spectrum of **3** shows a base peak at m/z 146 corresponding to [M − CO$_2$]$^+$. A molecular ion cannot be obtained due to decarboxylation. Upon adding CF$_3$COOH or concentrated HCl to a solution of **3** in polar solvents, the color of the solution changes from red-brown to yellow; the NMR spectrum indicates the presence of indandione only, obtained as a result of the decarboxylation of **3**.

Compound **3** is insoluble in nonpolar solvents. It is soluble in dimethylformamide and DMSO with a red-brown color. The

SCHEME 2

SCHEME 3

an1   **an2**
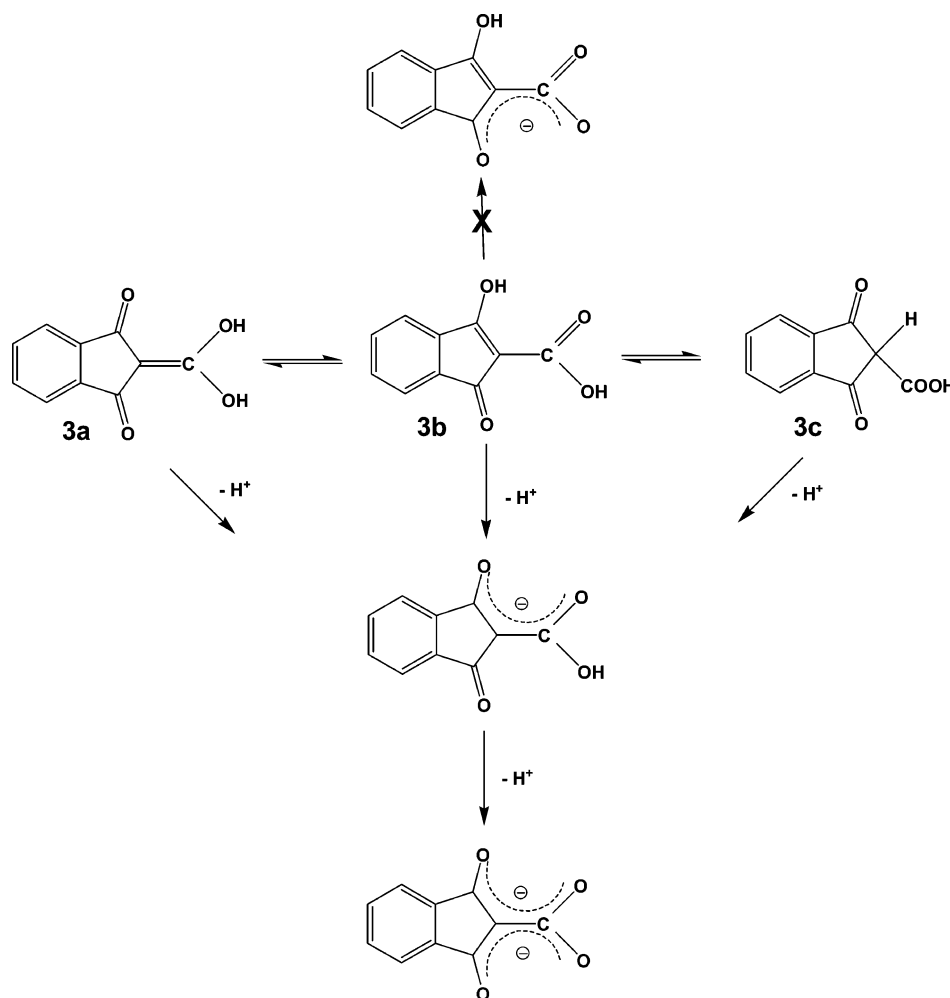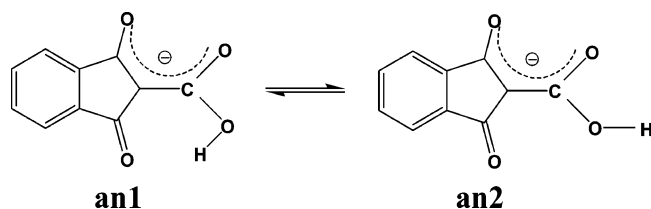
solubility in tetrahydrofuran, acetone, methanol, and water is low; however the initial yellowish suspension of **3** in these solvents turns to a red-brown solution within ca. 30 min. Most probably the red-brown color of the solution is an indication of the formation of the anionic form or a mixture of anion and dianion (Scheme 2).[34]

Only one anionic form can be obtained from the three tautomeric forms **3a**−**c**. For this anion two rotamers are possible, with (**an1**) and without (**an2**) an intramolecular hydrogen bond (Scheme 3). The rotamer **an1** is more stable than **an2**; the Gibbs free energy difference is 8.54 and 6.94 kcal mol^{-1} at the MP2 level using the 6-31G** and 6-31+G** basis sets, respectively.

The MP2-calculated bond lengths and selected torsion angles for tautomers **a**, **b**, and **c** and the anion and dianion of **3** are summarized in Table 9. The extension of the basis set from 6-31G** to 6-31+G** for the anions leads to a weak lengthening of all carbonyl bonds by 0.002−0.005 Å and carbon−carbon bonds by 0.002−0.004 Å. The C6−C7 and C5−C7 bonds shorten by 0.02 Å. The formation of dianion from anion leads to the following changes: strong lengthening of the C9−C10

bond by 0.1 Å and shortening of the C7−C9 and C8−C9 bonds by 0.01 Å. The dianion has a nonplanar structure; the carboxy group is almost perpendicular to the indandione moiety, at angles of 82° and 88°, depending on the optimization level, MP2/6-31G** and MP2/6-31+G**, respectively.

In Table 10 are listed the experimental and calculated (with and without taking into account the solvent effect) chemical shifts of tautomers **3a**−**c** (Figure 1), the anions (two rotameric forms), and the dianion of compound **3**. It can be seen that the inclusion of solvent effects through PCM leads to no improvement in the values of the calculated carbon chemical shifts. The calculated chemical shifts of tautomer **c**, whose presence in solution is excluded by the experimental ^{13}C NMR spectra, are presented for comparison with the chemical shifts of the anion and dianion of compound **3**. By analysis of the average deviation between calculated and experimental values of chemical shifts, it can be seen that the calculated values for **an2** are closest to experiment ($\Delta\delta = 0.9$ ppm in the gas phase and 2.0 ppm in DMSO solution). The average deviations for **an1** are $\Delta\delta = 1.4$ ppm in the gas phase and 2.5 ppm in DMSO solution. Probably the anion and/or the dianion of compound **3** exist in solution. The calculated chemical shifts of tautomer **b** are also close to the experimental ones with average deviations of $\Delta\delta = 1.7$ ppm in the gas phase and 2.3 ppm in DMSO solution.

Interestingly, the chemical shifts of the carbonyl oxygen atoms change more than those of the hydroxyl ones when one passes from the gas phase to DMSO solution. A measurement of the experimental ^{17}O NMR spectrum of **3** is desirable to

elucidate the reproduction of experimental values by calculation in the gas phase and in solution. The ^{17}O chemical shifts could be used to identify the structure(s) in solution because of the fact that they diverge greatly for different tautomers and anions.

The analysis of IR spectra was performed by comparing the experimental spectra with the theoretical ones, using both frequency and intensity matching as guidelines for the assignments. The IR spectra of **3** in CH_2Cl_2 and CH_3CN are presented in Figure 6. The observed carbonyl frequency modes in CH_2-Cl_2 at 1713, 1701, 1692, 1671, and 1637 cm^{-1} correspond to frequency modes at 1715, 1671, and 1632 cm^{-1} in CH_3CN. A possible equilibrium between two forms may be inferred from the strong frequency shift of C=O stretching modes in the more polar solvent. One form can be related to tautomer **3b**. The other is an anionic form. Similar to the anionic form tautomer **3b** can also exist as two rotamers. The rotamer without an intramolecular hydrogen bond **3b1** is less stable. The MP4/6-31G**//MP2/6-31G**-calculated Gibbs free energy difference between **3b** and **3b1** is 2.47 kcal mol^{-1}. Selected calculated vibrational frequencies of rotameric forms **3b** and **3b1** and of the rotameric anions (**an1** and **an2**) and experimental frequency modes are presented in Table 11.

The observed in CH_2Cl_2 frequency modes at 1701 and 1692 cm^{-1} could be assigned to tautomer **3b** (Table 11). Its carbonyl frequency modes are calculated at 1706 cm^{-1} ($\nu(C10=O12)$) and 1662 cm^{-1} ($\nu(C7=O18)$). The formation of anion shifts the $\nu(C10=O12)$ band up to 1735 cm^{-1}, the $\nu(C7=O18)$ band disappears, and two new bands arise: $\nu^s(C=O)$ at 1650 cm^{-1} and $\nu^{as}(C=O)$ at 1605 cm^{-1}. The carbonyl bands, which are characteristic of an anion, are found at 1713, 1671, and 1637 cm^{-1}. A similar spectral behavior was observed in the formation of 2-phenyl-indane-1,3-dione anion.[34] In the more polar solvent, CH_3CN, the tautomer−anion equilibrium is strongly shifted to the anionic form. The corresponding carbonyl modes of the anion are observed at 1715, 1671, and 1632 cm^{-1} (Table 11). Increase of the solvent polarity leads to changes in the band intensity of the carbonyl modes that strongly overlap each other (Figure 6).

The observed frequency modes at 3640 and 3540 cm^{-1} in CH_3CN $\nu(OH)$ correspond to a hydroxyl group uninvolved in hydrogen bonding. The first one could be assigned to the anion form **an2**, and the second one to tautomer **3b1** (Table 11). The calculated values for $\nu(OH)$ of a hydroxyl group involved in hydrogen bonding are low, 3176−3191 cm^{-1}.

TDDFT B3LYP/aug-cc-pVDZ calculations were performed to predict the absorption maxima of the tautomers and the anionic forms of compound **3**. The calculated $\pi-\pi^*$ electron transitions for the anionic forms **an1** and **an2** are presented in Figure 7. The experimental observed low-intensive long-wavelength absorption bands in ethanol at about 26 500 and 31 500 cm^{-1} prove the existence of **an1** and/or **an2** in solution.

4. Conclusions

The paper studies the tautomerism of the following 2-substituted 1,3-indandiones: 2-formyl-indan-1,3-dione, 2-acetyl-indan-1,3-dione, 2-carboxyindan-1,3-dione, and 2-carboxyamide-indan-1,3-dione. We show that for 2-formyl-indan-1,3-dione and 2-acetyl-indan-1,3-dione the equilibrium is shifted toward tautomer **a** in the gas phase and in solution, while 2-carboxy-amide-indan-1,3-dione exists as a mixture of tautomers **4a** and **4b** with extremely fast proton transfer between them. The situation for 2-carboxy-indan-1,3-dione is more complicated. According to the gas-phase-calculated Gibbs free energy differences of tautomers **3a**, **3b**, and **3c** obtained at the MP2/6-

31G** level, tautomer **3b** is favored. At the MP4/6-31G**//MP2/6-31G** and PCM/MP4/6-31G**//MP2/6-31G** levels, **3c** is predicted to be the most stable; however its existence in solution is not confirmed experimentally. On the basis of the results obtained, it can be concluded that in solution 2-carboxy-indan-1,3-dione exists in anionic form.

References and Notes

(1) (a) Toullec, J. In *The Chemistry of Enols*; Rappoport, Z., Ed.; Wiley: Chichester, U. K., 1990; p 323. (b) Forsén, S.; Nilson, M. In *The Chemistry of the Carbonyl Group*; Zabicky, J., Ed.; Interscience Publishers: New York, 1970; Vol. 2, p 198. (c) Neylands, O. In *Structure and Tautomerism of β-Dicarbonyl Compounds*; Gudrience, E., Ed.; Zinatne: Riga, Latvia, 1976; p 142.

(2) (a) Iglesias, E. *J. Phys. Chem.* **1996**, *100*, 12592. (b) Iglesias, E. *J. Chem. Soc., Perkin Trans. 2* **1997**, 431. (c) Iglesias, E. *New J. Chem.* **2005**, *29*, 457. (d) Iglesias, E. *J. Phys. Chem. B* **2001**, *105*, 10287.

(3) (a) Iglesias, E.; Ojea-Cao, V.; Garcia-Rio, L.; Leis, J. R. *J. Org. Chem.* **1999**, *64*, 3954. (b) Iglesias, E. *J. Org. Chem.* **2000**, *65*, 6583. (c) Iglesias, E. *J. Inclusion Phenom. Macrocyclic Chem.* **2005**, *52*, 55.

(4) Iglesias, E. *Curr. Org. Chem.* **2004**, *8*, 1.

(5) Enchev, V. *Chem. Pap.* **1994**, *48*, 219.

(6) (a) Hassal, C. H. *Experientia* **1950**, *6*, 462. (b) Hazleton, L. W.; Dolben, W. H. U. S. Patent 2,884,357, 1959. (c) Correll, J. T.; Coleman, L. L.; Long, St.; Willy, R. F. *Proc. Soc. Exp. Biol. Med.* **1952**, *80*, 139.

(7) Korp, J. D.; Bernal, I.; Lemke, T. L. *Acta Crystallogr., Sect. B* **1980**, *36*, 428.

(8) Petrova, M. V.; Liepins, E.; Paulins, J.; Gudele, I.; Gudriniece, E. *Izv. Akad. Nauk Latv. SSR, Ser. Khim.* **1987**, 601.

(9) Antipin, Yu. M.; Petrova, M. V.; Paulins, J. J.; Struchkov, Yu. T.; Gudriniece, E. Yu. *Izv. Akad. Nauk Latv. SSR, Ser. Khim.* **1989**, 102.

(10) Liepins, E.; Petrova, M. V.; Gudriniece, E.; Paulins, J.; Kuznetsov, S. L. *Magn. Reson. Chem.* **1989**, *27*, 907.

(11) Enchev, V.; Bakalova, S.; Ivanova, G.; Stoyanov, N. *Chem. Phys. Lett.* **1999**, *314*, 234.

(12) Gromak, V. V.; Avakyan, V. G.; Pashkovskii, F. S.; Lakhvich, O. F.; Skorodumov, E. V.; Khlebnikova, T. S. *J. Appl. Spectrosc.* **2003**, *70*, 16.

(13) Ahmedova, A.; Mantareva, V.; Enchev, V.; Mitewa, M. *Int. J. Cosmet. Sci.* **2002**, *24*, 103.

(14) Horton, R. L.; Murdock, K. C. *J. Org. Chem.* **1960**, *25*, 938.

(15) Enchev, V.; Abrahams, I.; Angelova, S.; Ivanova, G. *J. Mol. Struct. (THEOCHEM)* **2005**, *719*, 169.

(16) Michael, A.; Gabriel, S. *Berichte* **1877**, *10*, 391.

(17) Gabriel, S.; Neumann, A. *Berichte* **1893**, *26*, 951.

(18) Tirzîtis, G.; Žagats, R.; Vanags, G. *Latv. PSR Zinat. Akad. Vestis* **1962**, 97.

(19) PC Gamess Home Page. http://classic.chem.msu.su/gran/gamess/index.html.

(20) Schmidt, M. W.; Baldridge, K. K.; Boatz, J. A.; Elbert, S. T.; Gordon, M. S.; Jensen, J. H.; Koseki, S.; Matsunaga, N.; Nguyen, K. A.; Su, S.; Windus, T. L.; Dupuis, M.; Montgomery, J. A. *J. Comput. Chem.* **1993**, *14*, 1347.

(21) (a) Ditchfield, R.; Hehre, W. J.; Pople, J. A. *J. Chem. Phys.* **1971**, *54*, 724. (b) Hehre, W. J.; Ditchfield, R.; Pople, J. A. *J. Chem. Phys.* **1972**, *56*, 2257. (c) Hariharan, P. C.; Pople, J. A. *Theor. Chim. Acta* **1973**, *28*, 213.

(22) Krishnan, R.; Binkley, J. S.; Seeger, R.; Pople, J. A. *J. Chem. Phys.* **1980**, *72*, 650.

(23) Urban, J.; Schreiner, P. R.; Vacek, G.; Schleyer, P. V. R.; Huang, J. Q.; Leszczynski, J. *Chem. Phys. Lett.* **1997**, *264*, 441.

(24) Miertus, S.; Scrocco, E.; Tomasi, J. *Chem. Phys.* **1981**, *55*, 117.

(25) Miertus, S.; Tomasi, J. *Chem. Phys.* **1982**, *65*, 239.

(26) Frisch, M. J.; Trucks, G. W.; Schlegel, H. B.; Scuseria, G. E.; Robb, M. A.; Cheeseman, J. R.; Zakrzewski, V. G.; Montgomery, J. A., Jr.; Stratmann, R. E.; Burant, J. C.; Dapprich, S.; Millam, J. M.; Daniels, A. D.; Kudin, K. N.; Strain, M. C.; Farkas, O.; Tomasi, J.; Barone, V.; Cossi, M.; Cammi, R.; Mennucci, B.; Pomelli, C.; Adamo, C.; Clifford, S.; Ochterski, J.; Petersson, G. A.; Ayala, P. Y.; Cui, Q.; Morokuma, K.; Malick, D. K.; Rabuck, A. D.; Raghavachari, K.; Foresman, J. B.; Cioslowski, J.; Ortiz, J. V.; Stefanov, B. B.; Liu, G.; Liashenko, A.; Piskorz, P.; Komaromi, I.; Gomperts, R.; Martin, R. L.; Fox, D. J.; Keith, T.; Al-Laham, M. A.; Peng, C. Y.; Nanayakkara, A.; Gonzalez, C.; Challacombe, M.; Gill, P. M.

2-Substituted Indan-1,3-diones

J. Phys. Chem. A, Vol. 111, No. 39, 2007 **9913**

W.; Johnson, B. G.; Chen, W.; Wong, M. W.; Andres, J. L.; Head-Gordon, M.; Replogle, E. S.; Pople, J. A. *Gaussian 98*, revision A.7; Gaussian, Inc.: Pittsburgh, PA, 1998.

(27) Helgaker, T.; Jaszunski, M.; Ruud, K. *Chem. Rev.* **1999**, *99*, 293.

(28) Wolinski, K.; Hilton, J. F.; Pulay, P. J. *J. Am. Chem. Soc.* **1990**, *112*, 8251−8260.

(29) Frisch, M. J.; Trucks, G. W.; Schlegel, H. B.; Scuseria, G. E.; Robb, M. A.; Cheeseman, J. R.; Montgomery, J. A., Jr.; Vreven, T.; Kudin, K. N.; Burant, J. C.; Millam, J. M.; Iyengar, S. S.; Tomasi, J.; Barone, V.; Mennucci, B.; Cossi, M.; Scalmani, G.; Rega, N.; Petersson, G. A.; Nakatsuji, H.; Hada, M.; Ehara, M.; Toyota, K.; Fukuda, R.; Hasegawa, J.; Ishida, M.; Nakajima, T.; Honda, Y.; Kitao, O.; Nakai, H.; Klene, M.; Li, X.; Knox, J. E.; Hratchian, H. P.; Cross, J. B.; Bakken, V.; Adamo, C.; Jaramillo, J.; Gomperts, R.; Stratmann, R. E.; Yazyev, O.; Austin, A. J.; Cammi, R.; Pomelli, C.; Ochterski, J. W.; Ayala, P. Y.; Morokuma, K.; Voth, G. A.; Salvador, P.; Dannenberg, J. J.; Zakrzewski, V. G.; Dapprich, S.; Daniels, A. D.; Strain, M. C.; Farkas, O.; Malick, D. K.; Rabuck, A. D.; Raghavachari, K.; Foresman, J. B.; Ortiz, J. V.; Cui, Q.; Baboul, A. G.; Clifford, S.; Cioslowski, J.; Stefanov, B. B.; Liu, G.; Liashenko, A.; Piskorz, P.; Komaromi, I.; Martin, R. L.; Fox, D. J.; Keith, T.; Al-Laham, M. A.; Peng, C. Y.; Nanayakkara, A.; Challacombe, M.; Gill, P. M. W.; Johnson, B.; Chen, W.; Wong, M. W.; Gonzalez, C.; Pople, J. A. *Gaussian 03*, revision B.04; Gaussian, Inc.: Wallingford, CT, 2004.

(30) Casida, M. E.; Jamorski, C.; Casida, K. C.; Salahub, D. R. *J. Chem. Phys.* **1998**, *108*, 4439.

(31) (a) Becke, A. D. *J. Chem. Phys.* **1993**, *98*, 5648. (b) Lee, C. T.; Wang, W. T.; Pople, R. G. *Phys. Rev. B* **1988**, *37*, 785.

(32) (a) Woon, D. E.; Dunning, T. H., Jr. *J. Chem. Phys.* **1993**, *98*, 1358. (b) Kendall, R. A.; Dunning, T. H., Jr.; Harrison, R. J. *J. Chem. Phys.* **1992**, *96*, 6796.

(33) Enchev, V.; Ismailova, A.; Ivanova, G.; Wawer, I.; Stoyanov, N.; Mitewa, M. *J. Mol. Struct.* **2001**, *595*, 67.

(34) Kolev, Ts.; Velcheva, E.; Juchnovski, I. *Spectrochim. Acta, Part A* **1989**, *54*, 1083.

(35) Minchev, St.; Enchev, V.; Nedev, H. *Z. Naturforsch., B: Chem. Sci.* **1990**, *45*, 543.

(36) Foresman, J. B.; Keith, T. A.; Wiberg, K. B.; Snoonian, J.; Frisch, M. J. *J. Phys. Chem.* **1996**, *100*, 16098.